The Astrophysical Journal, 634:L161–L164, 2005 December 1


# RESOLVING THE Fe XXV TRIPLET WITH *CHANDRA* IN CENTAURUS X-3

R. Iaria,[1] T. Di Salvo,[1] N. R. Robba,[1] L. Burderi,[2] G. Lavagetto,[1] and A. Riggio[1]

*Received 2005 July 12; accepted 2005 October 21; published 2005 November 22*

## ABSTRACT

We present the results of a 45 ks *Chandra* observation of the high-mass X-ray binary Cen X-3 at orbital phases between 0.13 and 0.40 (in the eclipse post-egress phases). Here we concentrate on the study of discrete features in the energy spectrum at energies between 6 and 7 keV, that is, on the iron K$\alpha$ line region, using the High Energy Transmission Grating Spectrometer (HETGS) on board the *Chandra* satellite. We clearly see a K$\alpha$ neutral iron line at ~6.40 keV and were able to distinguish the three lines of the Fe XXV triplet at 6.61, 6.67, and 6.72 keV, with equivalent widths of 6, 9, and 5 eV, respectively. The equivalent width of the K$\alpha$ neutral iron line is 13 eV, an order of magnitude lower than previous measures. We discuss the possibility that the small equivalent width is due to a decrease of the solid angle subtended by the reflector.

*Subject headings:* line: formation — line: identification — pulsars: individual (Centaurus X-3) — X-rays: binaries — X-rays: general

*Online material:* color figures

## 1. INTRODUCTION

Centaurus X-3 is an X-ray pulsar with an O-type supergiant companion. The orbital period is ~2.1 days, and eclipses are observed. Out of eclipse, an iron emission line has been detected at $6.5 \pm 0.1$ keV (Nagase et al. 1992; Burderi et al. 2000). Nagase et al. (1992) suggested that the feature at 6.5 keV, observed in a *Ginga* spectrum, could be fitted by two Gaussian lines centered at 6.4 and 6.67 keV, with the latter stronger than the former during eclipse. The 6.5 keV line was found to be pulsating, supporting the fluorescence origin (Day et al. 1993) and implying that the fluorescence region does not uniformly surround the neutron star. Because of the large X-ray luminosity ($10^{37}$–$10^{38}$ ergs $s^{-1}$) and a strong stellar wind from the companion, Day & Stevens (1993) proposed that photoionization of the circumstellar wind by X-ray irradiation will be significant in the Cen X-3 system. Therefore, we expect the presence of emission lines due to recombination in highly ionized plasma. Ebisawa et al. (1996), using data from the *Advanced Satellite for Cosmology and Astrophysics* (*ASCA*) taken at different orbital phases, identified the presence of three emission lines centered around 6.40 keV (Fe I), 6.65 keV (Fe XXV), and 6.95 keV (Fe XXVI). The intrinsic width of each line was fixed at 0.01 keV, which was much smaller than the instrumental resolution. The equivalent widths (EWs) associated with the three lines were 105, 78, and 43 eV, respectively, at orbital phases between 0.14 and 0.18. Ebisawa et al. suggested that the line at 6.65 keV could be a blend of three lines at 6.63, 6.67, and 6.70 keV. The simultaneous presence of the Fe XXV and Fe XXVI lines in the spectrum implied an ionization parameter for the photoionized plasma of $\xi \sim 10^{3.4}$.

The common idea is that the K$\alpha$ neutral iron line is produced in a low-ionization region near the neutron star's surface, because this line is weaker during eclipse than out of eclipse. On the other hand, the Fe XXV and Fe XXVI lines are produced in a region far from the neutron star, probably in the photoionized wind of the companion star, because the intensities of these lines do not change with orbital phase.

Recently, Wojdowski et al. (2003), using *Chandra* data, analyzed the spectrum of Cen X-3 during eclipse. They resolved the Si XIII triplet and, in part, the Fe XXV triplet, concluding that the helium-like triplet component flux ratios outside of eclipse are consistent with emission from recombination and subsequent cascades (recombination radiation) from a photoionized plasma with a temperature of 100 eV. The best-fit velocity shifts and (Gaussian $\sigma$) velocity widths are generally less than 500 km $s^{-1}$. These velocities are significantly smaller than the terminal velocities of isolated O star winds [$(1–2) \times 10^3$ km $s^{-1}$; see, e.g., Lamers et al. 1999].

In this Letter, we present a spectral analysis of Cen X-3 in the 6–7 keV energy range from a 45 ks *Chandra* observation. The observation covers the orbital phase interval 0.13–0.40. We detect the presence of the K$\alpha$ neutral iron line at 6.4 keV, and for the first time, we resolve the triplet associated with the He-like ion of Fe XXV.

## 2. OBSERVATION

Cen X-3 was observed with the *Chandra* satellite on 2000 December 30 from 00:13:30 to 13:31:53 UT using HETGS. The observation has a total integration time of 45.3 ks and was performed in timed graded mode. HETGS consists of two types of transmission gratings, the Medium Energy Grating (MEG) and the High Energy Grating (HEG). HETGS affords high-resolution spectroscopy from 1.2 to 31 Å (0.4–10 keV) with a peak spectral resolution of $\lambda/\Delta\lambda \sim 1000$ at 12 Å for the HEG first order. The dispersed spectra were recorded with an array of six CCDs, which are part of the Advanced CCD Imaging Spectrometer (Garmire et al. 2003). The current relative accuracy of the overall wavelength calibration is on the order of 0.05%, leading to a worst-case uncertainty of 0.004 Å in the MEG first order and 0.006 Å in the HEG first order. We processed the event list using available software (FTOOLS and CIAO ver. 3.2 packages). We computed aspect-corrected exposure maps for each spectrum, allowing us to correct for effects from the effective area of the CCD spectrometer.

The brightness of the source required additional efforts to mitigate "photon pileup" effects. A 349-row "subarray" (with the first row = 1) was applied during the observation, which reduced the CCD frame time to 1.3 s. The zeroth-order image is affected by heavy pileup: the event rate is so high that two

[1] Dipartimento di Scienze Fisiche ed Astronomiche, Università degli Studi di Palermo, via Archirafi 36, I-90123 Palermo, Italy; iaria@fisica.unipa.it.

[2] Dipartimento di Fisica, Università degli Studi di Cagliari, Strada Provinciale Monserrato-Sestu km 0.7, I-09042 Monserrato, Italy.

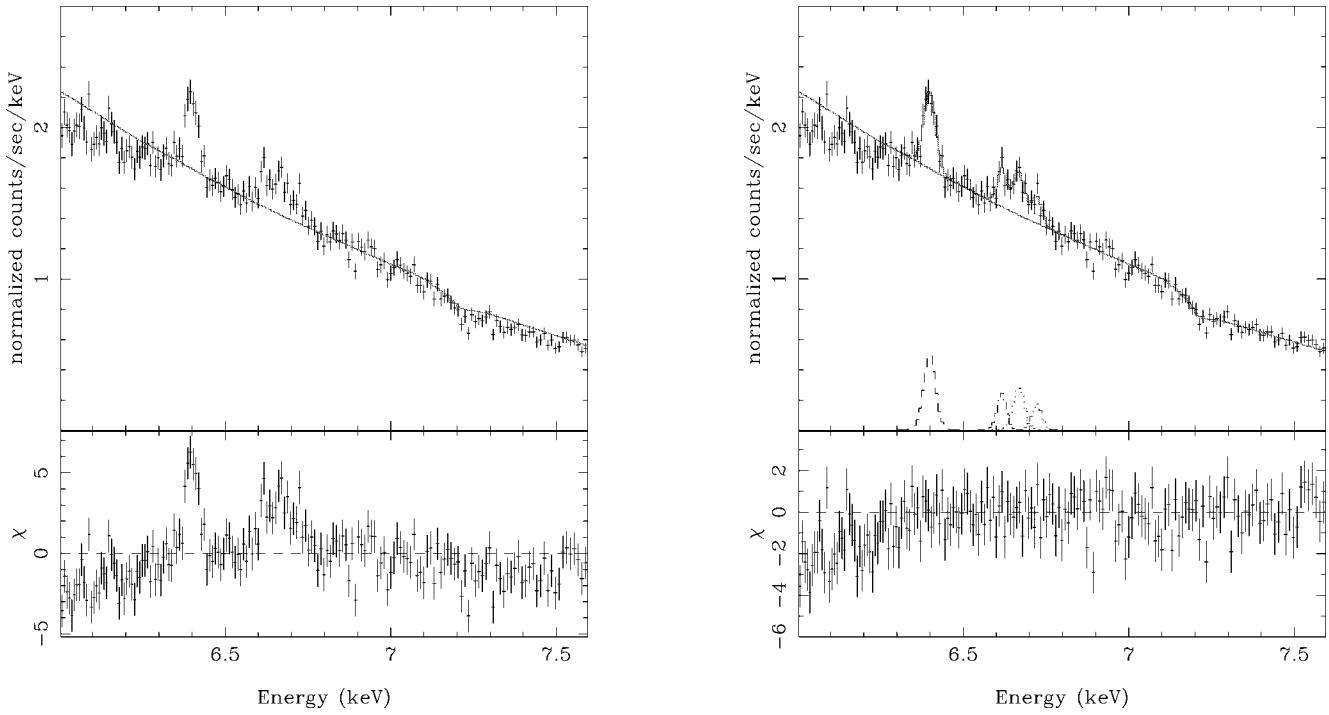


FIG. 1.—Data and residuals in the energy range 6.5–6.8 keV. *Left*: The continuum emission is modeled with a power-law component. Two features are clearly evident, at 6.4 and 6.65 keV, respectively. *Right*: The feature centered at 6.4 keV was modeled by a Gaussian line corresponding to the K$\alpha$ neutral iron line. The broad feature centered at 6.65 keV can be modeled by three Gaussian lines at 6.61, 6.67, and 6.72 keV, respectively, corresponding to the Fe XXV triplet. [*See the electronic edition of the Journal for a color version of this figure.*]

or more events are detected in the CCD during the 1.3 s frame exposure. Pileup distorts the count spectrum because detected events overlap and their deposited charges are collected into single, apparently more energetic, events. Moreover, many events (~90%) are lost, as the grades of the piled-up events overlap those of highly energetic background particles and are thus rejected by the onboard software. We therefore ignore the zeroth-order events in the subsequent analysis. On the other hand, the grating spectra are not or are only moderately (<10%) affected by pileup. In this work we use the HEG first-order spectrum to study the 6–7 keV energy range.

To determine the zero-point position in the image as precisely as possible, we calculated the mean crossing point of the zeroth-order readout trace and the tracks of the dispersed HEG and MEG arms. This results in the following source coordinates: R.A. = $11^h21^m15\overset{s}{.}095$, decl. = $-60°37'25\overset{''}{.}53$ (J2000, with a 90% uncertainty circle for the absolute position of $0\overset{''}{.}6$). Note that the *Chandra* position of Cen X-3 is ~$1\overset{''}{.}6$ distant from and fully compatible with the coordinates previously reported based on measurement of the optical counterpart (Bradt & McClintock 1983).

Finally, we used the ephemeris of Nagase et al. (1992) to determine which orbital phase interval was covered by our observation. The observation covers the phases between 0.13 and 0.40; it was taken just after egress from the eclipse, in the high, post-egress phase (see Nagase et al. 1992).

## 3. SPECTRAL ANALYSIS

We selected the first-order spectra from the HEG. Data were extracted from regions around the grating arms; to avoid overlapping between HEG and MEG data, we used a region size of 26 pixels for the HEG along the cross-dispersion direction. The background spectra were computed, as usual, by extracting data above and below the dispersed flux. The contribution from the background is 0.4% of the total count rate. We used the standard CIAO tools to create detector response files (Davis 2001) for the HEG first-order plus and minus (background-subtracted) spectra. After verifying that these two spectra were compatible with each other in the whole energy range, we co-added them using the script "add_grating_spectra" in the CIAO software; the resulting spectrum was rebinned to 0.0075 Å. Initially we fitted the 6–8 keV energy spectrum corresponding to the whole observation (orbital phases $\phi_{\rm orb} = 0.13$–$0.40$) using a power-law component as the continuum. We fixed the equivalent hydrogen column to $N_{\rm H} = 1.95 \times 10^{22}$ cm$^{-2}$ and the photon index to 1.2, as obtained by Burderi et al. (2000) from a *BeppoSAX* observation taken at similar orbital phases. The absorbed flux was ~$6.5 \times 10^{-9}$ ergs cm$^{-2}$ s$^{-1}$ in the 2–10 keV energy band, similar to the $5.7 \times 10^{-9}$ ergs cm$^{-2}$ s$^{-1}$ observed by Burderi et al. (2000) and 1 order of magnitude larger than that measured by *ASCA* at orbital phase 0.14–0.18 (~$8.4 \times 10^{-10}$ ergs cm$^{-2}$ s$^{-1}$; see Ebisawa et al. 1996). In Figure 1 (*left*), we show the spectrum and the residuals with respect to this model in the 6–7.6 keV energy range. Evident are the presence of a K$\alpha$ neutral iron emission line at 6.4 keV with a width of 0.012 keV and an absorption edge at 7.19 keV associated with low-ionization iron (Fe II–Fe VI). We note that near 6.65 keV a more complex structure is present in the residuals; three peaks can be seen. For this reason, we used three Gaussian lines to fit these residuals. The energies of the lines are 6.61, 6.67, and 6.72 keV, with corresponding widths less than 0.018, 0.023, and 0.037 keV; finally, the corresponding EWs are 6, 8.8, and 4.8 eV. In the right panel of Figure 1, we show the data and the residuals in the 6–7.6 keV energy range after adding the emission lines described above.

We note in the left panel of Figure 2 the presence of a feature at 2 keV. We fitted this feature using two Gaussian lines centered at 2 and 2.006 keV (corresponding to Si XIV Ly$\alpha_2$ and Ly$\alpha_1$, respectively). The widths of these two lines are around

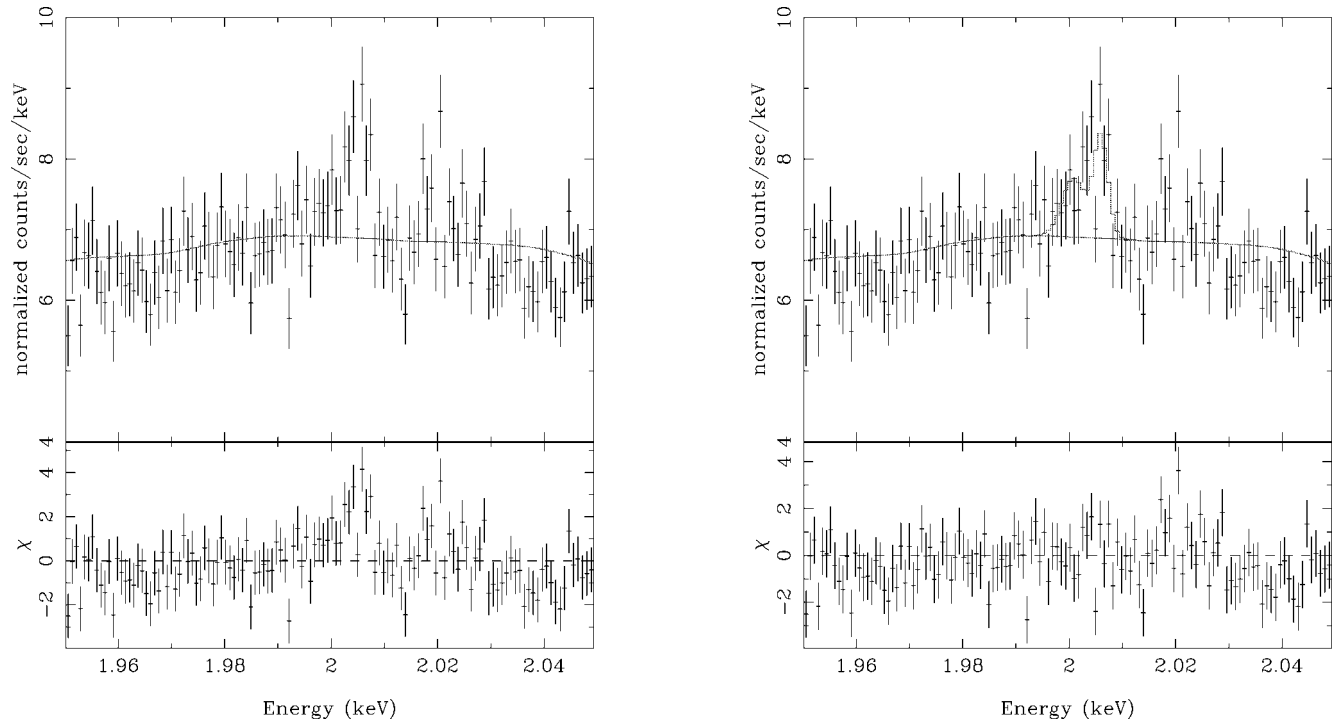


FIG. 2.—Data and residuals in the energy range 1.95–2.05 keV. *Left*: A broad feature is present at 2 keV. *Right*: The feature centered at 2 keV was modeled by two Gaussian lines corresponding to Si XIV Ly$\alpha_1$ and Ly$\alpha_2$. [*See the electronic edition of the Journal for a color version of this figure.*]

2 eV. In Table 1, we report the parameters of the emission lines and the absorption edge.

The EW of the neutral iron K$\alpha$ line is ~13 eV, lower by factors of 8 and 14 than the EWs of the neutral iron K$\alpha$ line obtained during *ASCA* (Ebisawa et al. 1996) and *Ginga* (Nagase et al. 1992) observations taken in the egress and post-egress phases, respectively, in which the unabsorbed flux of the continuum emission in the 2–10 keV energy range was $\sim 1 \times 10^{-9}$ and $\sim 4 \times 10^{-9}$ ergs cm$^{-2}$ s$^{-1}$, respectively. It is a common idea that the line at 6.4 keV is produced in the inner region of the system and that during dips and eclipses its flux decreases in proportion to the flux of the continuum, leaving the EW of the line unchanged at ~100 eV.

In light of these results, we have reanalyzed the previous *Chandra* observation (start time 2000 March 5) of Cen X-3 during the pre-eclipse phases (between $-0.16$ and $-0.12$), already studied by Wojdowski et al. (2003) and corresponding to "interval b" in their work (see Fig. 1 of Wojdowski et al. 2003). We fitted the first-order MEG and HEG data using a power-law component absorbed by an equivalent hydrogen column density fixed to $1.95 \times 10^{22}$ cm$^{-2}$ and by a partial-covering component with an equivalent hydrogen column density of $(1.2 \pm 0.4) \times 10^{23}$ cm$^{-2}$ and a covered fraction of the emitting region of 85% ± 6%. The photon index of the power law was 0.43, and the unabsorbed flux in the 2–10 keV energy band was $\sim 1.8 \times 10^{-9}$ ergs cm$^{-2}$ s$^{-1}$. As already discussed by Wojdowski et al., this spectrum shows a neutral iron K$\alpha$ emission line at 6.384 ± 0.013 keV with a width $\sigma < 39$ eV, a normalization of $9.4 \times 10^{-4}$ photons cm$^{-2}$ s$^{-1}$, and an EW of 42 ± 17 eV. As was done by Ebisawa et al. (1996) for the spectrum during the pre-eclipse state, we added the lines centered at 6.67 and 6.97 keV associated with Fe XXV and Fe XXVI, fixing the

TABLE 1
RESULTS OF THE SPECTRAL FIT

| Parameter | Phase Interval 0.13–0.40 | Parameter | Phase Interval 0.13–0.40 | Parameter | Phase Interval 0.13–0.40 | Parameter | Phase Interval 0.13–0.40 |
|---|---|---|---|---|---|---|---|
| Continuum | | K$\alpha$ Neutral Iron Line | | Fe XXV Intercombination (*i*) Line | | Si XIV Ly$\alpha_1$ Line | |
| $N_{\rm H}$ ($10^{22}$ cm$^{-2}$) ..... | 1.95 (fixed) | $E$ (keV) ..... | $6.3975^{+0.0033}_{-0.0033}$ | $E$ (keV) ..... | $6.6665^{+0.0067}_{-0.0036}$ | $E$ (keV) ..... | $2.0008^{+0.0063}_{-0.0032}$ |
| Photon index ..... | 1.2 (fixed) | $\sigma$ (keV) ..... | $0.0115^{+0.0045}_{-0.0042}$ | $\sigma$ (keV) ..... | <0.023 | $\sigma$ (keV) ..... | $0.00175^{+0.00290}_{-0.00071}$ |
| $N_{\rm po}$ ..... | 0.812 (fixed) | $I$ ($10^{-3}$ cm$^{-2}$ s$^{-1}$) ..... | $1.18^{+0.19}_{-0.17}$ | $I$ ($10^{-4}$ cm$^{-2}$ s$^{-1}$) ..... | $7.6^{+2.2}_{-3.0}$ | $I$ ($10^{-4}$ cm$^{-2}$ s$^{-1}$) ..... | $2.3^{+1.0}_{-1.2}$ |
| | | EW (eV) ..... | $13.2^{+2.1}_{-1.9}$ | EW (eV) ..... | $8.8^{+2.6}_{-3.5}$ | EW (eV) ..... | $0.64^{+0.29}_{-0.32}$ |
| Fe II–Fe VI Absorption Edge | | Fe XXV Forbidden (*f*) Line | | Fe XXV Resonance (*r*) Line | | Si XIV Ly$\alpha_2$ Line | |
| $E$ (keV) ..... | $7.189^{+0.024}_{-0.041}$ | $E$ (keV) ..... | $6.6129^{+0.0072}_{-0.0041}$ | $E$ (keV) ..... | $6.720^{+0.010}_{-0.022}$ | $E$ (keV) ..... | $2.0059^{+0.0400}_{-0.0021}$ |
| $\tau$ ..... | 0.079 ± 0.018 | $\sigma$ (keV) ..... | <0.018 | $\sigma$ (keV) ..... | <0.037 | $\sigma$ (keV) ..... | <0.0019 |
| | | $I$ ($10^{-4}$ cm$^{-2}$ s$^{-1}$) ..... | $5.2^{+2.1}_{-1.6}$ | $I$ ($10^{-4}$ cm$^{-2}$ s$^{-1}$) ..... | $4.2^{+2.9}_{-1.8}$ | $I$ ($10^{-4}$ cm$^{-2}$ s$^{-1}$) ..... | $2.53^{+1.06}_{-0.81}$ |
| | | EW (eV) ..... | $6.0^{+2.5}_{-1.8}$ | EW (eV) ..... | $4.8^{+3.3}_{-2.0}$ | EW (eV) ..... | $0.71^{+0.29}_{-0.23}$ |

NOTES.—The model is composed of a power-law with absorption from neutral matter. Uncertainties are at the 90% confidence level for a single parameter; upper limits are at the 95% confidence level. $N_{\rm po}$ indicates the normalization of the power-law component in units of photons keV$^{-1}$ s$^{-1}$ cm$^{-2}$ at 1 keV. The parameters of the Gaussian emission lines are $E$, $\sigma$, $I$, and EW, indicating the centroid, the width, the intensity of the line in units of photons cm$^{-2}$ s$^{-1}$, and the equivalent width, respectively.

centroids at the expected values and the widths to 10 eV. We found upper limits on the line intensities of $\sim 4.2 \times 10^{-4}$ and $\sim 2.1 \times 10^{-4}$ photons cm$^{-2}$ s$^{-1}$; moreover, the inferred EW upper limits are 22 and 11 eV, respectively, for the Fe XXV and Fe XXVI emission lines. We conclude that these results are in absolute agreement with those reported by Ebisawa et al. (1996). However, the relatively low value (42 eV) of the EW of the neutral iron K$\alpha$ emission line is indeed intermediate between the value measured by *ASCA* (75 eV) and the one we measure with *Chandra* (13 eV) and might indicate a trend of decreasing EW in 2000.

## 4. DISCUSSION

We have analyzed a 45 ks *Chandra* observation of the high-mass X-ray binary Cen X-3. The position of the zeroth-order image of the source provides improved X-ray coordinates for Cen X-3 (R.A. = $11^h21^m15\overset{s}{.}095$, decl. = $-60°37'25\overset{''}{.}53$), compatible with the optical coordinates previously reported for this source (Bradt & McClintock 1983). We performed a spectral analysis of the HEG first-order spectra of Cen X-3. The continuum emission is well fitted by a power-law component with a photon index of 1.2 absorbed by an equivalent hydrogen column density fixed at $1.95 \times 10^{22}$ cm$^{-2}$. The inferred unabsorbed flux is $\sim 7.4 \times 10^{-9}$ ergs cm$^{-2}$ s$^{-1}$ in the 2–10 keV energy band, corresponding to a luminosity of $5.6 \times 10^{37}$ ergs s$^{-1}$ in the 2–10 keV energy band, assuming a distance to the source of 8 kpc (Krzemiński 1974). We detected a complex structure in the X-ray spectrum at 6–7.6 keV, in particular, a K$\alpha$ neutral iron emission line at 6.4 keV with a width of 12 eV, significantly different from zero and corresponding to a velocity dispersion of 1270 km s$^{-1}$. We also resolved the triplet of Fe XXV at about 6.6–6.7 keV. Furthermore, we detected an absorption edge associated with Fe II–Fe VI.

We can explain the broad width of the K$\alpha$ neutral iron line by assuming that it was produced in an accretion disk. In fact, supposing that the width of the line was produced by a thermal velocity dispersion, then $T_4 \sim v^2/(2.89\ \mathrm{K})$, where $T_4$ is the temperature in units of $10^4$ K and $v$ is the velocity dispersion in kilometers per second. Since $v \sim 1270$ km s$^{-1}$ for the K$\alpha$ neutral iron line, the corresponding temperature should be $T \sim 5.6 \times 10^9$ K, physically not acceptable. On the other hand, assuming that the broadening is produced by the Keplerian motion of the accretion disk, we can infer the radius $r = (GM/c^2)(\Delta E/E)^{-2}$ where the line is produced; we find the inner radius of the reflecting region to lie between $8.3 \times 10^9$ and $5.5 \times 10^{10}$ cm, assuming for the source an inclination angle of $75^{+12}_{-13}$ deg (see Nagase 1989). This radius is compatible with the upper limit of $3.4 \times 10^{10}$ cm for the emission region of the K$\alpha$ neutral iron line given by Nagase et al. (1992) and Day et al. (1993). Therefore, we conclude that the most probable origin of the 6.4 keV line is reflection from the outer accretion disk.

As noted in § 3, the low value of the EW of the 6.4 keV line measured in the *Chandra* observations of 2000 March and December might indicate that there is a trend of decreasing EW of the 6.4 keV line component in 2000. A possible explanation of the low EW observed during our observation might involve changes in the geometry of the reflector. Perhaps the solid angle subtended by the reflector with respect to the illuminating source changes with time (from $2\pi$ to less), maybe as a result of precession of the accretion disk.

For the first time, thanks to the high energy resolution of *Chandra*, we were able to resolve the 6.6 keV line in the Cen X-3 spectrum as three lines centered at 6.61, 6.67, and 6.72 keV with EWs of 6, 9, and 5 eV. The Fe XXV He-like triplet is potentially a powerful diagnostic tool of density and temperature. We find that the intensities of the intercombination ($i$), resonance ($r$), and forbidden ($f$) lines are $7.6 \times 10^{-4}$, $4.2 \times 10^{-4}$, and $5.2 \times 10^{-4}$ photons cm$^{-2}$ s$^{-1}$, respectively. We find that $R \equiv f/i$ and $G \equiv (f + i)/r$ are $0.68 \pm 0.39$ and $3.05 \pm 2.25$ (where the uncertainties are at the 90% confidence level for a single parameter). As Bautista & Kallman (2000) point out, caution should be exercised with the use of $R$ and $G$ as density and temperature diagnostics, respectively, since they are sensitive to whether the plasma is collisionally ionized or photoionized. Nevertheless, the temperature curves of Bautista & Kallman indicate that $T$ is between either $6.3 \times 10^5$ and $1.5 \times 10^7$ K or $10^7$ and $4 \times 10^7$ K, for collisional and photoionized gas, respectively. Because in the case of Cen X-3 (a bright X-ray source emitting near the Eddington limit) we are probably dealing with photoionized gas, we can conclude that the temperature of the emitting region is $(1–4) \times 10^7$ K. Furthermore, the density curves are consistent with $n_e < 10^{17}$ cm$^{-3}$. Although we obtain a weak upper limit on the electron density, this is compatible with the typical stellar wind density of $n_e = 10^{10}$–$10^{11}$ cm$^{-3}$.

Finally, we note that we did not see the Fe XXVI line at 6.9 keV that was observed in the previous *ASCA* observation (Ebisawa et al. 1996). This implies that the stellar wind had, during our observation, a lower ionization parameter than the $\xi \sim 10^{3.4}$ estimated by Ebisawa et al. We estimate that $\xi$ should be $\sim 10^{2.6}$–$10^{2.8}$ (see Fig. 7 of Ebisawa et al. 1996). This is also compatible with the detection of Si XIV Ly$\alpha$ at 2 keV. From $\xi = L_X/n_e^2 d$ (see Krolik et al. 1981), assuming a source luminosity of $L_X \sim 1.3 \times 10^{38}$ ergs s$^{-1}$ in the 0.1–200 keV energy band (see Burderi et al. 2000), an ionization parameter $\xi \simeq 10^{2.6}$–$10^{2.8}$, and a separation between the neutron star and the companion star of $d \simeq 10^{12}$ cm (Nagase et al. 1992), we find an electron density of the emitting region of $2 \times 10^{11}$ cm$^{-3}$, in agreement with the previous results and compatible with the upper limit obtained above.

We thank the referee for useful suggestions. This work was partially supported by the Italian Space Agency (ASI) and the Ministero della Istruzione, della Universitá e della Ricerca.

## REFERENCES

Bautista, M. A., & Kallman, T. R. 2000, ApJ, 544, 581
Bradt, H. V. D., & McClintock, J. E. 1983, ARA&A, 21, 13
Burderi, L., Di Salvo, T., Robba, N. R., La Barbera, A., & Guainazzi, M. 2000, ApJ, 530, 429
Davis, J. E. 2001, ApJ, 562, 575
Day, C. S. R., Nagase, F., Asai, K., & Takeshima, T. 1993, ApJ, 408, 656
Day, C. S. R., & Stevens, I. R. 1993, ApJ, 403, 322
Ebisawa, K., Day, C. S. R., Kallman, T. R., Nagase, F., Kotani, T., Kawashima, K., Kitamoto, S., & Woo, J. W. 1996, PASJ, 48, 425
Garmire, G. P., Bautz, M. W., Ford, P. G., Nousek, J. A., & Ricker, G. R., Jr. 2003, Proc. SPIE, 4851, 28
Krolik, J. H., McKee, C. F., & Tarter, C. B. 1981, ApJ, 249, 422
Krzemiński, W. 1974, ApJ, 192, L135
Lamers, H. J. G. L. M., Haser, S., de Koter, A., & Leitherer, C. 1999, ApJ, 516, 872
Nagase, F. 1989, PASJ, 41, 1
Nagase, F., Corbet, R. H. D., Day, C. S. R., Inoue, H., Takeshima, T., Yoshida, K., & Mihara, T. 1992, ApJ, 396, 147
Wojdowski, P. S., Liedahl, D. A., Sako, M., Kahn, S. M., & Paerels, F. 2003, ApJ, 582, 959 (erratum 607, 1071 [2004])